Analysis of an Airplane Windshield Anti-Icing System Using Hot Air

R. Ross*
Ross Aviation Associates, Sedgwick, Kansas

This paper documents the analysis methods developed to predict the performance of the windshield hot air anti-icing system on a business jet airplane. Flight data gathered from dry air and natural icing tests are used to develop and verify the accuracy of a procedure that will predict the windshield surface temperature for either wet or dry air. It is shown that windshield surface temperatures can be estimated to an accuracy of ±5% for a wide range of aircraft conditions. It is demonstrated that the method is somewhat conservative for all conditions.

Nomenclature

alt	= altitude, ft
D_D	= median droplet diameter, μm
f,g	= functions in Eq. (2)
K_1,K_2	= constants in Eq. (4)
LWC	= liquid water content, g/m^3
P	= pressure, psf
T	= temperature, °R
T_w	= windshield surface temperature, °R
V	= velocity, ft/s
VKIAS	= indicated airspeed, knots
W_B	= bleed air mass flow rate to windshield, lb/s
X	= distance along windshield, ft
η	= ordinate for thermocouple location, in.
ξ	= abscissa for thermocouple location, in.

Subscripts

A	= ambient
B	= bleed air
D	= droplet
L	= liquid water content
0	= dry air

Introduction

THE properties of similitude are used to analyze dry air and natural icing flight test data for the windshield anti-icing system of a business jet airplane. The results of this analysis are then used to formulate a method for predicting the windshield surface temperature for any known aircraft flight and icing conditions.

Sufficient data were available to be able to account for the effects of variations in both liquid water content and water droplet diameter. The relative humidity in these icing tests is assumed to be 100%.

Evaluation of the method is performed by comparing calculated and measured windshield surface temperatures for a variety of conditions. Comparison of measured surface temperature data obtained during dry air and natural icing conditions with calculated surface temperatures for the same flight conditions indicates that the accuracy is within ±5% and the method tends to be somewhat conservative; i.e., calculated temperatures tend to be somewhat cooler than measured temperatures.

Presented as Paper 82-1372 at the AIAA 7th Atmospheric Flight Mechanics Conference, San Diego, Calif., Aug. 9-11, 1982; submitted Aug. 9, 1982; revision received Feb. 22, 1983.

*Director.

Development of the Prediction Model

The use of similitude in developing a mathematical model for analyzing the performance of hot airflow anti-icing systems for aircraft windshields is reported in Ref. 1. General information on the anti-icing analysis is contained in Refs. 2-4. The model used in the data analysis of this report is an extension of that of Ref. 1 to include accountability for the effects of droplet size and liquid water content as variables in the analysis.

Similitude permits the reduction of the number of parameters or variables in the problem. The dependent and independent quantities affecting windshield surface temperature are as follows:

1) Bleed air mass flow
2) Bleed air temperature
3) Bleed air pressure
4) Ambient temperature
5) Ambient pressure
6) Aircraft airspeed
7) Position on the windshield
8) Water droplet diameter
9) Liquid water content

It is desirable to distinguish the dependent variable from the independent quantities and to express the dependent variable, the windshield surface temperature T_w, as a function of the independent variables, i.e.,

$$T_w = f(W_B, T_B, P_B, T_A, P_A, V, X, D_D, \mathrm{LWC}) \tag{1}$$

It is noted that both water droplet size and liquid water content are included as independent variables. At this stage in the analysis both of these variables will be eliminated from the list and reintroduced at a later stage in the development. Thus,

$$T_w = f(W_B, T_B, P_B, T_A, P_A, V, X) + g(D_D, \mathrm{LWC}) \tag{2}$$

where the effects of function f will be evaluated during the first stage of analysis and the effects of function g will be evaluated in the final stage of analysis.

Following the procedure of similitude it is shown[1] that the dependent and independent variables of the function f can be reduced to three dimensionless products that have a functional relation given by

$$T_W/T_A = f(W_B V/X^2 P_A, T_B/T_A) \tag{3}$$

The form of the unknown function f is not revealed by the dimensional anlaysis but it will be derived from the analysis of test data. Similarly, the effects of the unknown function g will be derived from test data.

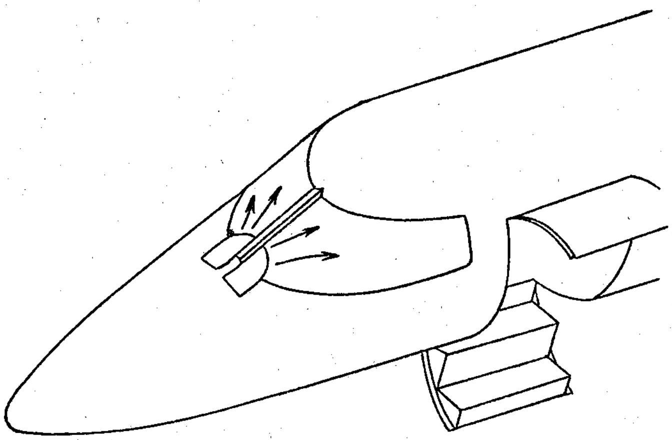

Fig. 1 Windshield anti-icing system.

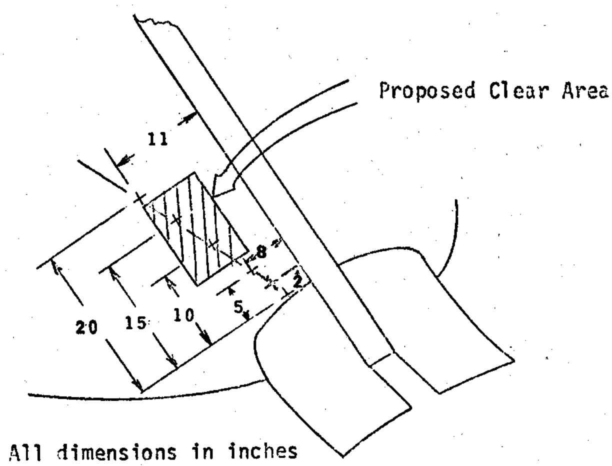

Fig. 2 Location of thermocouples.

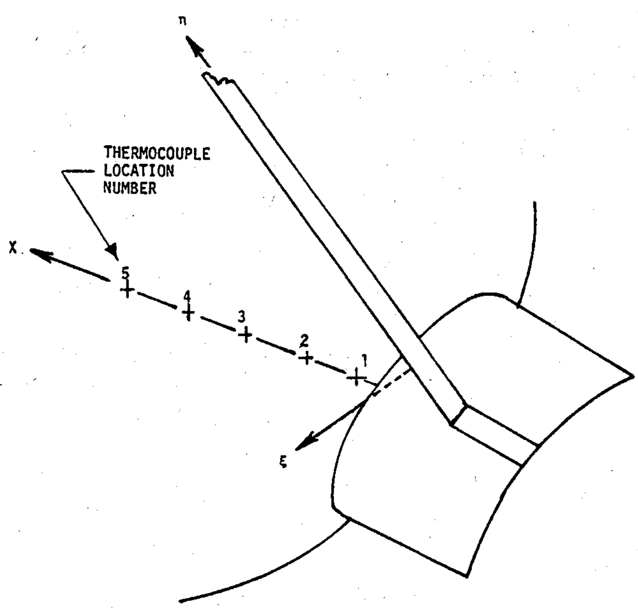

Fig. 3 Thermocouple location geometry.

Table 1 Distance to thermocouples

Thermocouple No.	η, in.	ξ, in.	X, in.
1	7.4	2	2.00
2	8	5	5.04
3	9	10	10.13
4	10	15	15.22
5	11	20	20.32

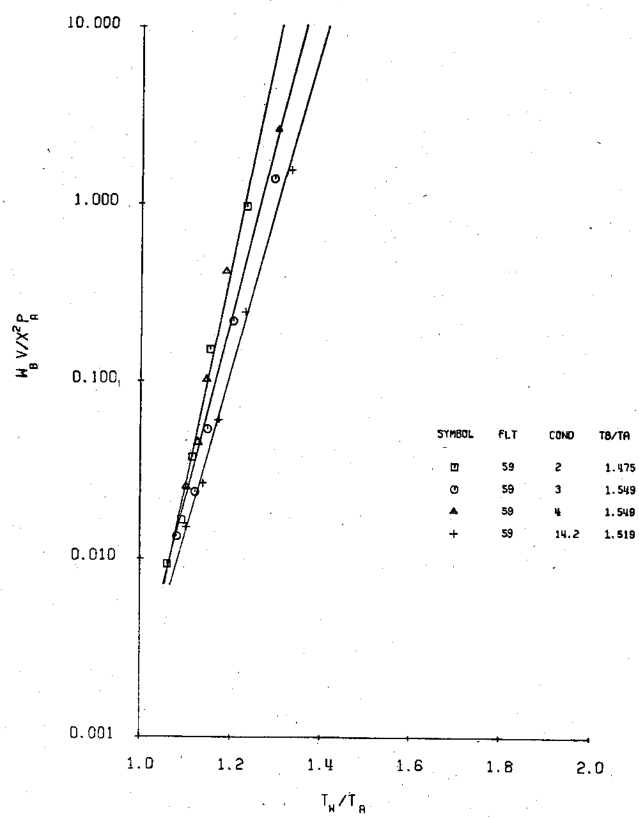

Fig. 4 Typical data plot.

Test Procedure

Flight tests were conducted on an instrumented airplane. Hot air for anti-icing is obtained as bleed from the aircraft engines and is supplied to the windshield through a duct exiting at the center of the lower side of the windshield as shown in Fig. 1. Five thermocouples were bonded to the windshield at the locations shown in Fig. 2. Also shown is a proposed clear area for adequate pilot vision. This is a rectangular area 9 in. wide and 12 in. high located 6 in. from the windshield center bar and 7 in. above the nozzle exit. The size and location of this area was determined by pilot comments and FAA requirements to provide a satisfactory clear area for pilot vision during icing conditions. The thermocouples are located so that they run diagonally through the clear area box. The reference axis system for location of the thermocouples and determination of the reference distance X used in the analysis is shown in Fig. 3. The origin of this axis system is located at the intersection of the side of the windshield center bar and the lower side of the bleed air exit duct. Tabulated values of the coordinates and X are presented in Table 1.

Test data were recorded for a variety of flight conditions as shown in Table 2 for both dry air and natural icing environment.

Data Analysis

Five test flights with dry air and five test flights with a wide range of natural icing conditions were flown. The mean droplet diameter and liquid water content for all test conditions were measured for use in this analysis. The test data were reduced to the three dimensionless groups indicated by Eq. (3) and plotted on semilog graph paper as illustrated in Fig. 4. Inspection of the data indicates that there are sets of data points corresponding to nearly constant values of T_B/T_A. Straight lines can be faired through these sets as shown. Least-squares linear regression analysis is used to fit straight lines to the data.

In order to determine a uniform family of lines fitting the data and conforming to Eq. (3), and to expand the range of

Table 2 Flight test conditions

Condition	Range
Altitude, 1000 ft	5-45
Ambient temperature, °F	−81-51
Airspeed, knots	153-349
Bleed flow, lb/min	3.9-10.7
Bleed temperature, °F	239-345
Droplet diameter, μm	5-33
Liquid water content, g/m^3	0.02-0.35

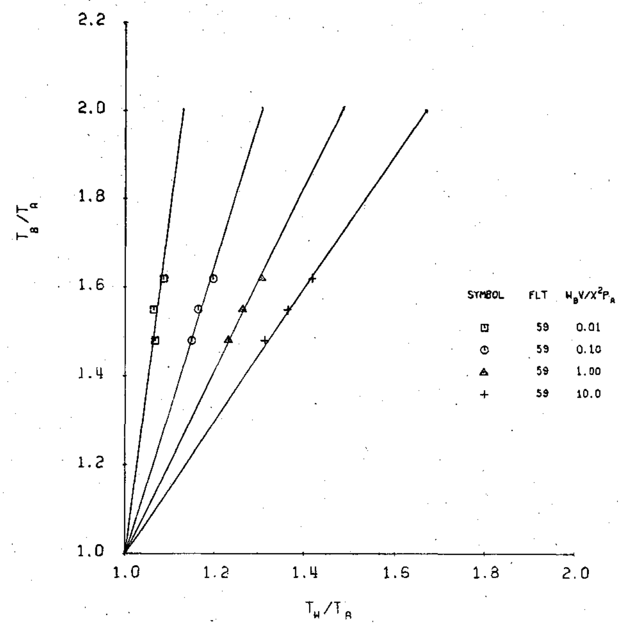

Fig. 5 Typical data crossplot.

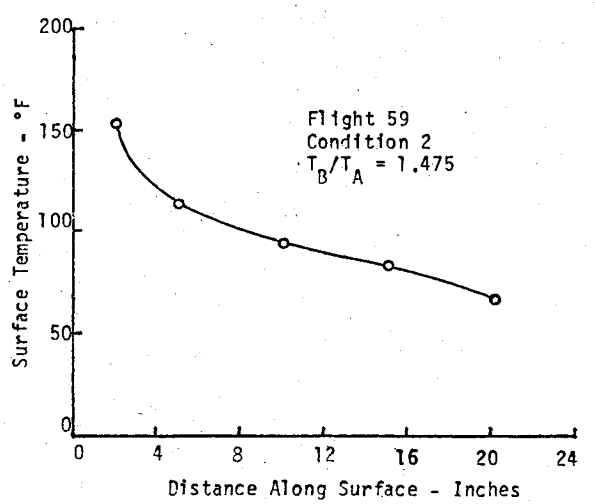

Fig. 6 Typical surface temperature distribution.

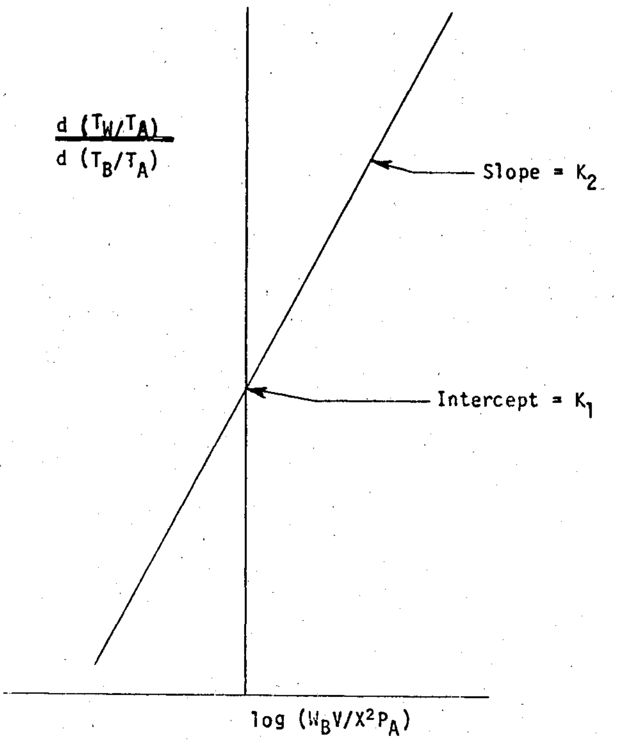

Fig. 7 Definition of the constants K_1 and K_2.

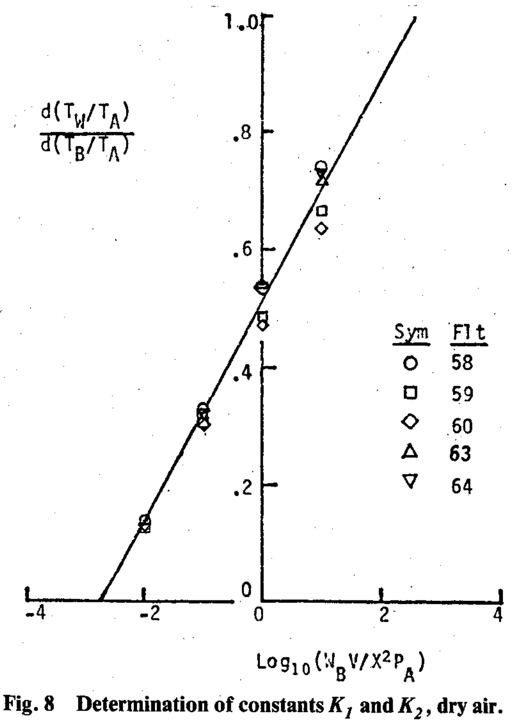

Fig. 8 Determination of constants K_1 and K_2, dry air.

application from the measured data, it is helpful to prepare crossplots of the data of Fig. 4. Plots of T_B/T_A vs T_W/T_A for discrete values of $W_B V/X^2P_A$ are prepared (Fig. 5) in order to give a better definition of the family of lines in Fig. 4. Straight lines are drawn through the points in Fig. 5 using the knowledge that, with only slight error, the lines must pass through the origin. Crossplots of the data are made both for dry air and natural icing. For the natural icing analysis, these data are grouped by median droplet diameter. Least-squares linear regression analysis is used to fit straight lines to the data.

Further inspection of the data points in Fig. 4 and 5 reveals that the numerical equation that represents the function of Eq. (3) must have the form

$$T_W/T_A = 1.0 + [K_1 + K_2 \log_{10}(W_B V/X^2P_A)] \times (T_B/T_A - 1.0) \tag{4}$$

Local windshield surface temperatures required to derive values for the two constants K_1 and K_2 were measured during the test flights. A typical surface temperature distribution is shown in Fig. 6.

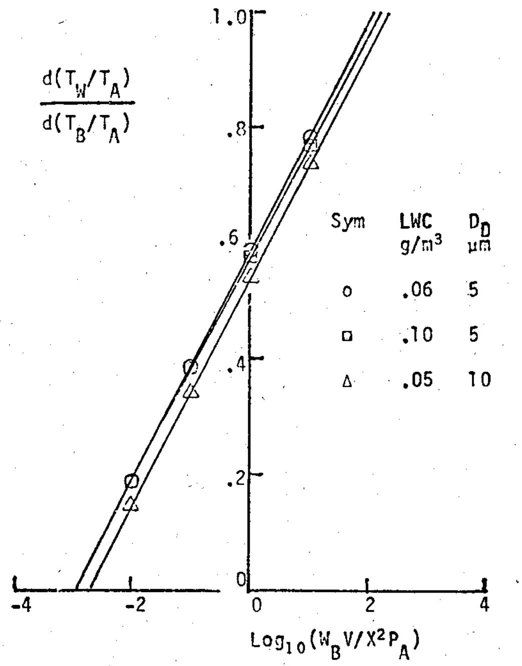

Fig. 9 Determination of constants K_1 and K_2, natural icing.

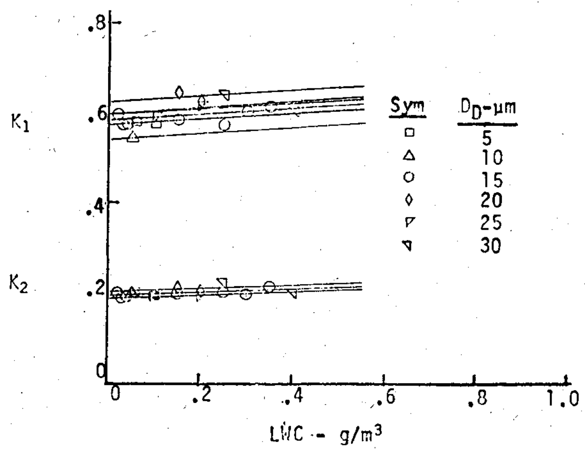

Fig. 10 Variation of constants K_1 and K_2 with liquid water content.

The derivative of Eq. (4) with respect to the bleed air temperature is

$$d(T_W/T_A)/d(T_B/T_A) = K_1 + K_2 \log_{10}(W_B V/X^2 P_A) \quad (5)$$

It is noted that this represents the slope of the lines in Fig. 5. Thus the values for K_1 and K_2 can be derived by plotting this slope, $d(T_W/T_A)/d(T_B/T_A)$, vs $\log(W_B V/X^2 P_A)$. Such a plot is illustrated in Fig. 7. In this plot the slope of the line represents K_2 and the intercept with the ordinate axis is K_1. Similar plots are made for dry air data (Fig. 8) and the natural icing data (Fig. 9). Linear regression analysis is used to fit a straight line to the data in Fig. 8. Values for K_1 and K_2 for the dry air are thus defined. Within the groups of data for similar droplet size there is considerable variation of liquid water content. Thus it is possible to determine the effects of both droplet size and liquid water content on K_1 and K_2. Figure 9 presents this data for two droplet diameters. Linear regression analysis is used to fit straight lines to the data. Values of K_1 and K_2, for each droplet size, as a function of liquid water content are presented in Fig. 10. Linear regression analysis is used to fit straight lines to this data and to obtain the slope of the lines, representing the effects of liquid water content (K_{1_L} and K_{2_L}), as well as the ordinate intercept, defining the effects of droplet size for zero liquid water content. This latter data is then plotted as a function of droplet size as shown in Fig. 11. Linear regression analysis is used to fit straight lines to the data. The derived values of K_1 and K_2 from the dry air analysis are included in Fig. 11 since all of this data, in theory, is for a liquid water content of zero. Linear regression analysis is used to determine a base value, K_{1_0} and K_{2_0}, at the intercept with the ordinate axis, $D_D = 0$, as well as the effects of droplet size on these constants, K_{1_D} and K_{2_D}, given by the slope of the lines.

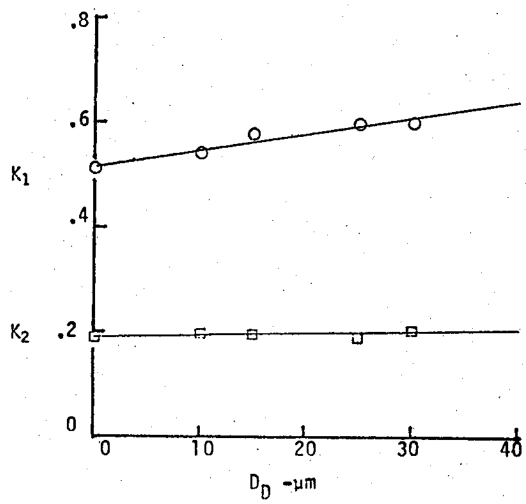

Fig. 11 Variation of constants K_1 and K_2 with droplet size, LWC = 0.

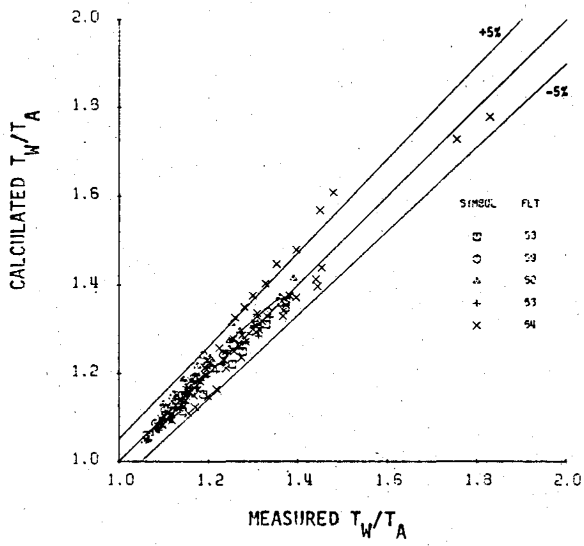

Fig. 12 Computational accuracy, dry air.

It is assumed, and verified by the analysis, that the effects of both droplet size and liquid water content are additive, i.e.,

$$K_1 = K_{1_0} + K_{1_D} + K_{1_L} \qquad K_2 = K_{2_0} + K_{2_D} + K_{2_L} \quad (6)$$

Thus

$$K_1 = 0.5131 + 0.003135\, D_D + 0.06808\, \mathrm{LWC}$$

$$K_2 = 0.1902 + 0.003793\, D_D + 0.003974\, \mathrm{LWC} \quad (7)$$

These relations for K_1 and K_2 along with the general relation for the surface temperature from Eq. (4) complete the data analysis.

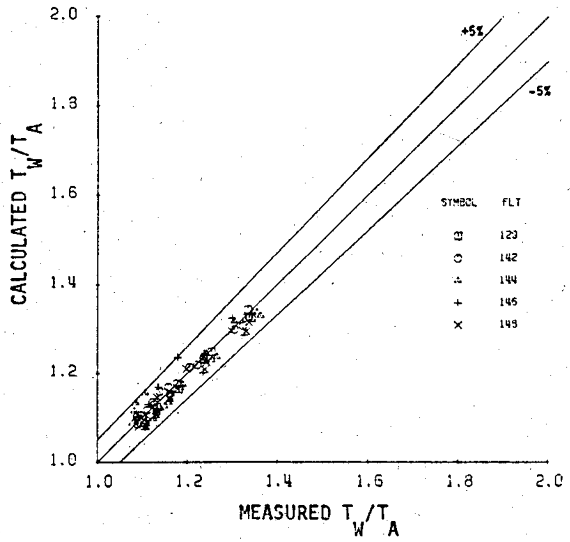

Fig. 13 Computational accuracy, natural icing.

Discussion of Results

The test of the validity of such a technique as derived is to calculate the value of the windshield surface temperature based on known test conditions and compare that value to the corresponding measured value. This was done for all of the available test data and the results are presented in Figs. 12 and 13 for dry air and natural icing, respectively. Shown are calculated and measured values of T_w/T_A. Error bands of $\pm 5\%$ are shown and the accuracy is excellent for all conditions. The prediction accuracy for dry air (Fig. 12) is generally within $\pm 5\%$ of measured data and there appears to be some conservatism in the calculation method.

It is noted that some of the calculated surface temperatures differ from the measured values by as much as 8.8%. Inspection of the data correlation plots (Figs. 4 and 5) for these conditions shows that there is poor correlation with respect to the balance of the data for these test flight conditions. Although it is not evident from the flight test data, it is obvious that there is probably something wrong with some of the flight test information supplied for these two conditions. They are not considered in the regression analysis used in Fig. 5 and should not be considered as valid data points for the comparison with calculated values.

The prediction accuracy for the natural icing tests (Fig. 13) is generally within $\pm 3\%$ of measured data. However, it is apparent that the calculation method tends to be generally conservative as compared to measured results. Thus one would expect that much more of the windshield will be clear of ice than indicated by computed results. This was verified by pilot observations during the natural icing test where nearly the total aircraft windshield was clear for even the most severe icing encounter. It is noted that the demonstrated accuracy of this method ($\pm 5\%$) may be due in part to the relatively small effects that liquid water content and droplet diameter have on the calculated values of K_1 and K_2. A contributing factor may be relatively poor accuracy of instrumentation available to measure liquid water content and droplet size.

Conclusions

The formulation of an accurate method for calculating the windshield surface temperatures for business jet airplanes for any type of icing conditions has been accomplished. It provides for the effects of droplet size and liquid water content and requires only information about aircraft, atmospheric and hot bleed air conditions.

For all of the tested conditions the accuracy is within $\pm 5\%$ or less of the measured values of surface temperature. The method tends to be conservative when compared to measured data for the conditions of natural icing. Thus the anti-icing system should maintain a larger clear area on the windshield than indicated by the calculated surface temperature profiles.

Acknowledgment

The author expresses appreciation to the Gates Learjet Corporation for their cooperation in releasing the data for publication.

References

[1] Ross, R., "Use of Similitude in Analyzing Aircraft Anti-icing Performance," *Journal of Aircraft*, Vol. 17, Nov. 1980, pp. 830-832.

[2] "Transport Category Airplanes, Appendix C," Federal Aviation Regulations, Airworthiness Standards, Part 25, Federal Aviation Administration, Washington, D.C., 1982.

[3] Heinrich, A., Ross, R., and Ganesan, N., "Engine Inlet Anti-icing System Evaluation Procedure," Federal Aviation Administration, Washington, D.C., FAA-RD-80-50, Jan. 1980.

[4] Bowden, D. T., Gensemer, A.E., and Skeen, C.A., "Engineering Summary of Airframe Icing Technical Data," Federal Aviation Administration, Washington, D.C., Tech. Rept. ADS-4, March 1964.